

Estimation of citrus canker lesion size using hyperspectral reflectance imaging

Nikhil P. Niphadkar^{1*}, Thomas F. Burks², Jianwei Qin³, Mark A. Ritenour⁴

(1. ATW Automation Inc., Dayton, OH 45402, USA;

2. Department of Agricultural and Biological Engineering, University of Florida, Gainesville, FL 32611, USA;

3. U.S. Department of Agriculture, Beltsville, MD 20705, USA;

4. Department of Horticultural Sciences, University of Florida, Gainesville, FL 34945, USA)

Abstract: The Citrus industry has need for effective approaches to remove fruit with canker before they are shipped to selective international market such as the European Union. This research aims to determine the detectable size limit for cankerous lesions using hyperspectral imaging approaches. Previously developed multispectral algorithms using visible to near-infrared wavelengths, were used to segregate cankerous citrus fruits from other peel conditions (normal, greasy spot, insect damage, melanose, scab and wind scar). However, this previous work did not consider lesion size. A two-band ratio method with a simple threshold based classifier (ratio of reflectance at wavelengths 834 nm and 729 nm), which gave maximum overall classification accuracy of 95.7%, was selected for lesion size estimation in this study. The smallest size of cankerous lesion detected in terms of equivalent diameter was 1.66 mm. The effect of variation of threshold values and number of erosion cycles (applying morphological erosion multiple times to the image) on estimation of smallest detectable lesion was observed. It was found that small threshold values gave better canker classification accuracies, while exhibiting a lower overall classification accuracy. Meanwhile, higher threshold values portrayed the opposite tendency. The threshold value of 1.275 gave the optimum tradeoff between canker classification accuracy, overall classification accuracy and minimal lesion size detection. Increasing the number of erosion cycles reduced detection rates of smaller canker lesions, leading to the conclusion that a single erosion cycle gave the best size estimation results. The erosion kernel of the size 3 mm × 3 mm was used during the exploration.

Keywords: citrus canker, lesion size, disease detection, hyperspectral reflectance imaging, image classification, multispectral algorithm, size detection limit

DOI: 10.3965/j.ijabe.20130603.006

Citation: Niphadkar N P, Burks T F, Qin J W, Ritenour M A. Estimation of citrus canker lesion size using hyperspectral reflectance imaging. *Int J Agric & Biol Eng*, 2013; 6(3): 41–51.

1 Introduction

Citrus canker is a serious disease that can infect most commercial citrus varieties. Caused by bacterial pathogen *Xanthomonas axonopodis*, the disease is characterized by conspicuous, erumpent lesions on leaves,

stems, and fruit. Citrus canker originated in Southeast Asia-India, and it has spread to Japan, South and Central Africa, the Middle East, Australia, New Zealand, the Pacific Islands, South America, and Florida^[1]. Some areas of the world (e.g., South Africa, Australia, the Fiji Islands, Mozambique, and New Zealand) have eradicated

Received date: 2012-12-02 **Accepted date:** 2013-05-29

Biographies: **Thomas F. Burks**, Assistant Professor, Department of Agricultural and Biological Engineering, University of Florida, PO Box 110570, Gainesville, FL 32611, USA. Tel: (352) 392-1864 Ext. 225; Email: tburks@ufl.edu. **Jianwei Qin**, Research Scientist, U.S. Department of Agriculture, 10300 Baltimore Avenue, Beltsville, MD 20705, USA. Tel: (301) 504-

8450 Ext. 244; Email: jianwei.qin@ars.usda.gov. **Mark A. Ritenour**, Associate Professor, Department of Horticultural Sciences, University of Florida, 2199 South Rock Road Fort Pierce, FL 34945, USA. Tel: (772) 468-3922; Email: ritenour@ufl.edu.

***Corresponding author: Nikhil P. Niphadkar**, ATW Automation Inc., 313 Mound Street, Dayton, Ohio 45402, USA. Tel: (937) 516-5140. Email: nniphadkar@atwautomation.com.

citrus canker. Eradication programs have been implemented in infected areas such as Argentina, Uruguay, and Brazil, and Florida with varying degrees of success. Citrus canker can cause defoliation, blemished fruit, premature fruit drop, twig dieback, and tree decline. Due to its fast spread in Florida climates (especially due to hurricane winds), high damage potential, and massive impact on export trade, canker is still considered a serious disease that threatens citrus-growing areas.

Florida produces more than 70% of the citrus supply in the United States, and it is currently the only growing region in the U.S. that is affected by canker^[2]. The Citrus Canker Eradication Program (CCEP), initialized by the Florida Department of Agriculture and Consumer Services - Division of Plant Industry (FDACS-DPI) and the U.S. Department of Agriculture - Animal and Plant Health Inspection Service (USDA-APHIS) in mid-1990's, was an attempt to alleviate the consequences that canker would have on the Florida citrus industry, as well as to keep other U.S. citrus-producing areas (e.g., Texas and California) from being infected and harmed by this disease. Because canker exhibits endemic features in most infected regions, there is no universal treatment or prevention that could completely eradicate the disease in all the infected areas. The current emphasis has been on minimizing the level of the disease and preventing its further spread to the areas that are unaffected or were already eradicated^[3]. Recently, the Florida eradication program has been terminated since citrus canker is now considered endemic. In certain international canker-free markets, the presence of cankerous fruit in a shipment could result in the whole shipment being deemed unmarketable. It has been the common practice to detect citrus canker and eliminate the infected fruit before they go to the market.

In recent years, Florida had been the only US state under quarantine for citrus canker and therefore could not ship canker blemished fruit within the US or to other countries that block shipment of canker infected fruit. In the fall of 2009, USDA-APHIS issued a new ruling based on research which demonstrated that canker cannot be transmitted by infected fruit that had been treated with an appropriate disinfectant^[4]. The ruling lifts the within

US blockade and now allows free shipment of disinfected fruit. However, there still remain several international markets that have not lifted the ban on canker infected fruit to date.

Finding and removal of canker infected fruit is currently performed by human inspectors in the packing house, which is labor-intensive and expensive. Technologies that can efficiently identify citrus canker would assure fruit quality and safety, which would enhance the competitiveness and profitability of the citrus industry. In some cases, canker lesions are so small that they cannot be readily identified by human eyes. However, if these fruits are detected at the port of entry, the entire shipment could be rejected at some markets. A number of optical sensing techniques (e.g., machine vision and spectroscopy) have been investigated to detect citrus-related diseases, defects, and blemishes^[5], leaf diseases^[6], fruit surface defects^[7], fruit rottenness^[8] and citrus canker lesions^[9]. However, no significant efforts have been reported which attempt to evaluate the minimum detectable canker lesion size. The goal of this research was to determine the minimum size limit at which citrus canker lesions can be reliably detected for real time packing line applications. In recent years, hyperspectral and multispectral imaging techniques have been developed as useful tools for quality and safety evaluation of food and agricultural products^[3,10,11]. The hyperspectral imaging technique reported by Kim et al.^[10,11] acquires 2-D spatial information across a range of hyperspectral bands from 450 nm to 930 nm, which generates a 3-D image cube with 10 nm spectral resolution in 92 bands. Although this large amount of spectral information is useful for exploratory laboratory research, the hyperspectral cube contains significant redundant information leaving real-time image acquisition and processing impractical. Consequently, hyperspectral band selection is usually performed to reduce dimensionality and thus find an optimal subset of the 92 bands which enhances detection with ten or less significant wavelengths.

Recent studies^[2,3,9,12] have demonstrated that hyperspectral imaging technique coupled with appropriate image processing and classification methods [i.e., principal

component analysis (PCA) and spectral information divergence (SID)] provides a useful means for detecting canker lesions on citrus fruit. However, the full spectral information used by the PCA and SID algorithms would limit their applications in rapid on-line disease inspection due to the large amount of 3-D hyperspectral data. Hence, a technique was developed to select a set of hyperspectral bands for citrus canker detection using multispectral algorithms (detailed explained in Section 2.4) in which correlation analysis has been used to identify important wavelengths for citrus canker detection based on hyperspectral reflectance data^[9]. Once the significant wavelengths are identified, optical filters corresponding to the wavelengths were mounted on a multispectral imaging system and used in a real time single-lane packing line simulator application^[12]. The objective of the study reported in this manuscript was to determine the smallest lesion size detectable by the present multispectral segregation algorithm developed by Qin^[12].

2 Materials and methods

2.1 Citrus samples

Since grapefruit is one of the most susceptible citrus varieties to citrus canker, ruby red grapefruits with normal surface, canker, and five common peel blemish

conditions (i.e., greasy spot, insect damage, melanose, scab, and wind scar) were tested in this study. Color images typical for each peel condition are shown in Figure 1. Each peel condition exhibits different visually detectable symptoms. Greasy spot, melanose, and scab are all caused by fungi, which generate surface blemishes that are formed by infection on immature fruit during the growing season. Greasy spot produces small necrotic specks, with the affected areas brown to black in color and greasy in appearance. Melanose is characterized by scattered raised pustules which are dark brown to black in color. Scab appears as corky raised lesions usually with the color of light brown. Different from the fungal diseases, citrus canker is caused by bacteria, and it is featured with conspicuous dark lesions. Mostly circular in shape, canker lesions vary in size and they are superficial (up to 1 mm deep) on the fruit peel^[13]. Diameters of the canker lesions tested in this study were approximately in the range of 1-9 mm. Insect damage is characterized by irregular grayish tracks on the fruit surface, which are generated by larvae of leaf miners that burrow under the epidermis of the fruit rind. Wind scar, which is caused by leaves, twigs, or thorns rubbing against the fruit, is a common physical injury on the fruit peel, and the scar tissue is generally gray.

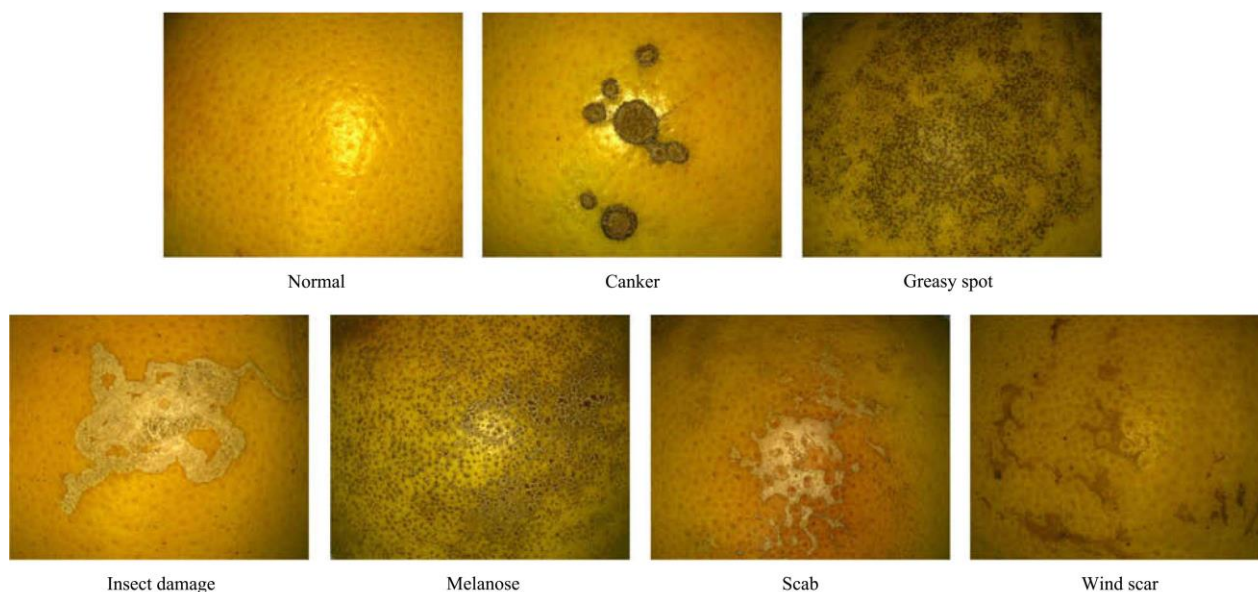


Figure 1 Representative normal and diseased grapefruit peel conditions demonstrating distinctive symptoms

Fruit samples were handpicked monthly from a grapefruit grove in Fort Pierce, Florida, during a

seven-month harvest period from Oct. 2007 to Apr. 2008. Thirty samples for each peel condition were collected for

each month, if the condition was available. Cankerous samples were collected all seven months, and the samples with other peel conditions were obtained every month according to their availability. Grapefruit samples exhibiting different sizes of canker lesions were used to evaluate the size detection limits for the hyperspectral

classification methods.

A total of 960 grapefruits were collected and tested in this study. The numbers of samples for each peel condition are summarized in Table 1, and were the same as those used in the study by Qin^[9].

Table 1 Numbers of fruit samples for each peel condition

Peel condition	Canker	Normal	Greasy spot	Insect damage	Melanose	Scab	Wind scar
Number	210	150	120	60	180	180	60

All grapefruit samples were washed and treated with chlorine and sodium o-phenylphenate (SOPP) at the Indian River Research and Education Center of University of Florida (UF) in Fort Pierce, Florida. The samples were transported to UF campus in Gainesville, Florida, and stored in an environmental control chamber maintained at 4 °C. The samples were removed from cold storage about two hours before imaging to allow them to reach room temperature. During image acquisition, the fruit samples were placed in rubber cups attached to the linear positioning table, with lesions facing upward, to insure that the diseased areas were in the imaging system's field of view.

2.2 Hyperspectral imaging system

A hyperspectral imaging system was used to acquire reflectance images from citrus samples. A schematic diagram of the system is illustrated in Figure 2. This hyperspectral imaging system was the same that was used by Qin^[3] and was developed in cooperation with the USDA Environmental Microbial and Food Safety Laboratory in Beltsville, MD, USA. The system is conceptually similar to the system reported by Kim^[10,11]. It is a push broom and line-scan based imaging system that utilizes an electron-multiplying charge-coupled-device (EMCCD) camera (iXon, Andor Technology Inc., South Windsor, CT, USA). The EMCCD has 1004×1002 pixels and is thermoelectrically cooled to negative 80 °C through a double-stage Peltier device. An imaging spectrograph (ImSpector V10E, Spectral Imaging Ltd., Oulu, Finland) and a C-mount zoom lens (Rainbow CCTV H6X8, International Space Optics, S.A., Irvine, CA, USA) are mounted to the camera.

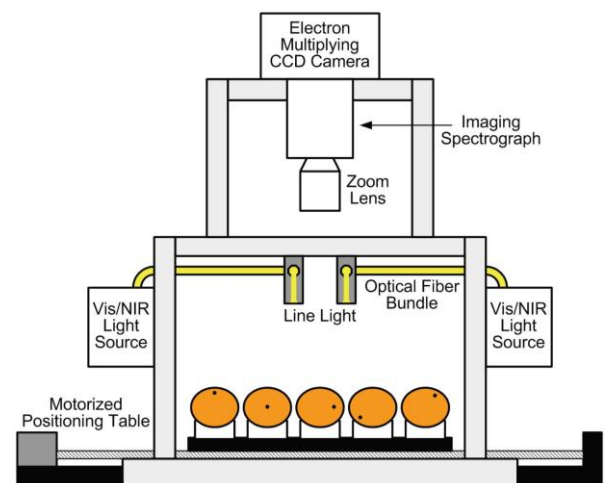


Figure 2 Hyperspectral imaging system for reflectance image acquisition from grapefruits

The instantaneous field of view (IFOV) is limited to a thin line by the spectrograph aperture slit (30 μm), and the spectral resolution of the imaging spectrograph is 2.8 nm. Through the slit, light from the scanned IFOV line is dispersed by a prism-grating-prism device and projected onto the EMCCD. Therefore, for each line-scan, a two-dimensional (spatial and spectral) image is created with the spatial dimension along the horizontal axis and the spectral dimension along the vertical axis of the EMCCD. The lighting unit consists of two 21 V, 150 W halogen lamps powered with a DC voltage regulated power supply (TechniQuip, Danville, CA, USA). The light is transmitted through optical fiber bundles toward line light distributors. Two line lights are arranged to illuminate the IFOV. A programmable, motorized positioning table (BiSlide-MN10, Velmex Inc., Bloomfield, NY, USA) moves citrus samples (five for each run) transversely through the line of the IFOV. 1740 line scans were performed for five fruit samples,

and 400 pixels covering the scene of the fruit at each scan were saved, generating a 3-D hyperspectral image cube with the spatial dimension of 1740×400 for each band. Spectral calibration of the system was performed using an Hg-Ne spectral calibration lamp (Oriel Instruments, Stratford, CT, USA). Because of inefficiencies of the system at certain wavelength regions (e.g., low light output in the visible region less than 450 nm, and low quantum efficiency of the EMCCD in the NIR region beyond 930 nm), only the wavelength range between 450 and 930 nm (totaling 92 bands with a spectral resolution of 5.2 nm) was used in this investigation. The parameterization and data-transfer interface software for the hyperspectral imaging system were developed using a SDK (Software Development Kit) provided by the camera manufacturer on a Microsoft Visual Basic (Version 6.0) platform in the Windows operating system.

2.3 Image pre-processing

As mentioned in the earlier section (Hyperspectral Imaging System), each hyperspectral image taken with our system consists of 3-D hyperspectral image cube with spatial dimension of 1740×400 and spectral dimension of 92 (92 wavelengths). To reduce the amount of data for computation, spatial binning technique^[21] was used in which the hyperspectral image data was averaged by two neighboring pixels in both vertical and horizontal spatial dimensions at each wavelength. This reduced the size of the original 3-D image data from $1740 \times 400 \times 92$ (92 bands) to $870 \times 200 \times 92$, and resulted in a spatial resolution of 0.6 mm/pixel for both vertical and horizontal dimensions. The image preprocessing procedures described above were executed using programs developed in MATLAB R2007a (Math Works, Natick, MA, USA).

Along with this, the image preprocessing was performed for the original hyperspectral reflectance images to fulfill flat-field correction and image masking which resulted in normalized and masked hyperspectral cubes with a dimension of $870 \times 200 \times 92$ (92 bands). Detailed procedures for hyperspectral image preprocessing can be found in the study by Qin^[21].

2.4 Hyperspectral band selection

The goal of this research was to determine the minimum size limit at which citrus canker lesions can be

reliably detected for real time packing line applications using an effective approach which segregates cankerous citrus fruits from normal peel or other surface defects. The citrus peel defect classification approach implemented in this study used a real-time multispectral algorithm based on correlation analysis for band selection^[9]. The hyperspectral imaging and band selection technique was a tool to identify the best wavelengths for segregating citrus canker. The reader should note that the hyperspectral imaging system itself was not employed on the real time segregation application. The optical filters, corresponding to the wavelengths identified using the hyperspectral band selection technique, were used in a multispectral real time single-lane packing line application.

Even after preprocessing the image data, the 3-D hyperspectral data ($870 \times 200 \times 92$) is still too large for real time applications and hence a multispectral algorithm is needed to reduce the computation time. The multispectral algorithm exploits correlation analysis (CA) to select the optimal pair of wavelengths in order to distinguish between canker, normal, and other diseased peel conditions. In this method, the selected pair is used to create a two band ratio image (i.e., $R_{\lambda_1}/R_{\lambda_2}$, where R_{λ_n} denotes single band reflectance image at the wavelength of λ_n) which helps us make the distinction. A ratio method was selected since ratio images are invariant to illumination scaling, a significant advantage for real-time applications. All 960 fruit samples were divided into two classes: 'Canker' class including 210 samples with canker lesions, and 'No Canker' class including 150 normal samples and 600 samples from five other peel diseases (Table 1). To facilitate correlation analysis, samples in the 'Canker' class were labeled '1', and 'No Canker' class was labeled '0'. Correlation coefficients were calculated between two band ratios for the region of interest (ROI) spectra for the two class labels (i.e., 1 and 0) in an exhaustive fashion (i.e., evaluating all possible two band combinations from the 92 wavelengths). The wavelength pair which had the maximum correlation coefficient became the optimum pair (previously mentioned earlier) and was selected for further classification of canker lesion size.

Keeping in mind that selecting additional wavelengths may (or may not) improve classification accuracies, the third and fourth bands were identified by performing the correlation analysis in a sequential forward way. The third band (i.e., R_{λ_3}) was determined by the highest correlation between the class label values and ratio values calculated as $(R_{\lambda_1} - R_{\lambda_3})/(R_{\lambda_2} - R_{\lambda_3})$, where R_{λ_1} and R_{λ_2} were two best bands selected from the previous correlation analysis. After the third band was determined, the fourth band was identified using the similar method on two forms of ratio calculations: $(R_{\lambda_1} - R_{\lambda_3})/(R_{\lambda_2} - R_{\lambda_{4a}})$ and $(R_{\lambda_1} - R_{\lambda_{4b}})/(R_{\lambda_2} - R_{\lambda_3})$, where R_{λ_1} , R_{λ_2} , and R_{λ_3} were determined from the previous procedures, and $R_{\lambda_{4a}}$ and $R_{\lambda_{4b}}$ were newly selected bands from the highest correlations. However, as demonstrated in previous studies^[9], the two band ratio method gives the best overall classification results and hence this study is an extension of the earlier two band ratio approach.

The two band ratio of 834 nm and 729 nm (R_{834}/R_{729}) was found to give the maximum absolute value for the correlation coefficient of 0.811 and hence was chosen to be the optimal pair of wavelengths to discriminate between fruit exhibiting cankerous and other peel conditions. The detailed procedure for selecting the optimal pair of wavelengths can be found in the study of Qin^[9].

2.5 Image classification

After identifying important wavelengths using CA, band ratio images were generated using ENVI 4.3 software (ITT Visual Information Solutions, Boulder, CO, USA) and the selected wavelength's single band images. The equation $R_{\lambda_1}/R_{\lambda_2}$ (i.e. R_{834}/R_{729}) was used to create these new ratio images.

A simple thresholding approach, which has been used to differentiate cancerous fruits from six other peel conditions (normal peel and other citrus diseases), was applied to the ratio images calculated using the above equations. A range of threshold values from 1.20 to 1.35 were evaluated to find the optimal classification accuracies for canker identification. A Morphological filtering operation was used prior to threshold-based classification in order to remove undesirable noise. Small pixel regions attributed to edge affects, minor peel

blemishes can result in an increase in false positives. However, there it is recognized that this filtering operation can also inhibit detection of very small canker lesions, and thus creates a tradeoff between the number of false positives, and false negatives. The morphological "opening" operation was used, which by definition means erosion of the image followed by subsequent dilation. The ENVI tools "opening" filter using a kernel size of 3×3 was selected. The purpose of erosion is to remove the undesirable small pixel groups recognized as noise, while the dilation smoothens out the contours of the remaining pixel areas to help restore the round features of the canker lesions in the final binary images. Then 30 samples from each peel condition were used to train the classifier. The threshold algorithm was then tested using the remaining samples of all the peel conditions.

2.6 Binary lesion size detection algorithm

In order to determine the smallest canker lesion detected using the above mentioned classification algorithm, the final binary images (after classification) were analyzed using a morphological opening operation. The function 'bwareaopen' in MATLAB R2007a (Math Works, Natick, MA, USA) was used to determine the number of pixels in the smallest canker lesion detected during the classification process. The function 'bwareaopen' removes all connected components (objects) from a binary image that have fewer than prescribed number of pixels defined in the syntax, thus producing another binary image. The number of pixels defined in the syntax was incremented by one at a time and the image before and after applying 'bwareaopen' function were compared for consistency. Whenever some difference was observed between the two images, the number of pixels (defined in syntax of 'bwareaopen') was noted. This pixel count minus one then represented the number of pixels (N') in the smallest canker lesion detected in the binary image by the lesion size estimation algorithm.

2.7 Mapping binary lesion size to original multispectral image

Once the smallest lesion size was obtained in the binary image, the actual smallest lesion size estimate could be found by mapping the lesion found in the binary

image back to the un-eroded lesion in the original multispectral image. This was done using ENVI. The X and Y coordinates of the centroid of smallest canker lesion in the classified binary image were estimated using MATLAB and the corresponding lesion in the original multispectral image was located. The number of pixels (N) in the original multispectral image lesion was counted using the region of interest (ROI) tool in Basic Tools of ENVI.

The spatial resolution of the images was 0.6 mm/pixel in horizontal direction and 0.6 mm/pixel in vertical direction. Hence the surface area of one pixel is $0.6 \times 0.6 \text{ mm}^2$. Accordingly, the surface area of the smallest canker lesion (A) was computed from the number of pixels in the lesion and area per pixel. Then assuming that most canker lesions are approximately circular in shape, the equivalent diameter (d) of the lesion was computed using the area of circle formula:

$$A = \pi d^2 / 4 \quad (1)$$

3 Results and discussion

3.1 Image classification

As demonstrated in a previous study^[9], it is not feasible to detect citrus canker using a single wavelength. Consequently, a multispectral imaging system was developed by selecting a wavelength subset from the 92 hyperspectral bands. The multispectral algorithm is illustrated in Figure 3 by showing the sequence of image processing steps which are necessary to generate the final thresholded binary image of a canker infected fruit. The original cankerous fruit image shown in Figure 3 is first masked, and then the two band ratio method (R_{834}/R_{729}) is applied to create the rule image. The threshold is then applied to obtain the binary image, and finally the morphological filter is applied to remove small noise pixels. The final binary image can then be examined to determine if canker pixels remain, thus classifying the fruit as cankerous. This sequence of images demonstrates the potential for small cankerous lesions to be removed along with undesired pixel noise during the erosion process. This can be observed in Figure 3, where two very small lesions in the 'Binary image' (image after Thresholding) disappeared after the

morphological opening operation in the final binary image. Although it is necessary to remove the pixel noise, the risk of removing small canker lesions during filtering can result in an increase in false negatives.

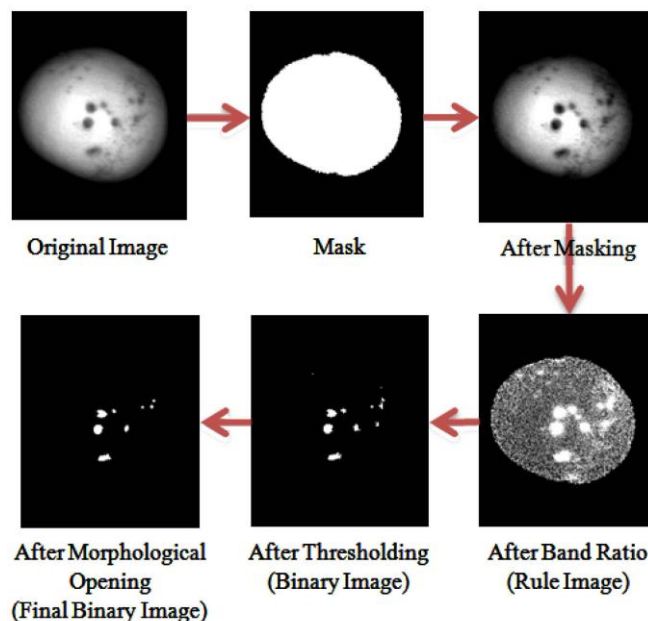


Figure 3 Image classification procedure demonstrating the six steps to isolate the canker lesions: 1) Create mask, 2) Masking image, 3) Band ratio, 4) Thresholding, 5) Morphological opening, and 6) Examine final image

Figure 4 demonstrates the algorithms ability to discriminate between canker and other peel conditions. The images shown in Figure 4 are mosaic images composed of seven peel condition samples which were generated to illustrate the algorithms ability to segregate canker from other conditions. As it can be seen in the final binary image (after morphological opening), white pixels appear only at canker lesions locations, while all other white pixels shown in the band ratio image were transformed to black.

The effect of varying threshold values on classification accuracy was analyzed for threshold values ranging from 1.20 to 1.35 for all two band ratio images. It was observed that the threshold value of 1.20 gave the best canker detection accuracy of 99.1% with an overall accuracy of 89.2%. Conversely, a higher threshold value of 1.35 did a better job in terms of the overall accuracy of 93.1%, but resulted in a significant reduction in canker detection accuracy to 77.6%. This can be attributed to the fact that as we increased the threshold

value, the smaller canker lesions were eliminated thus increasing the false negative errors. The result of variation of threshold value on classification accuracy can be easily observed from Figure 5.

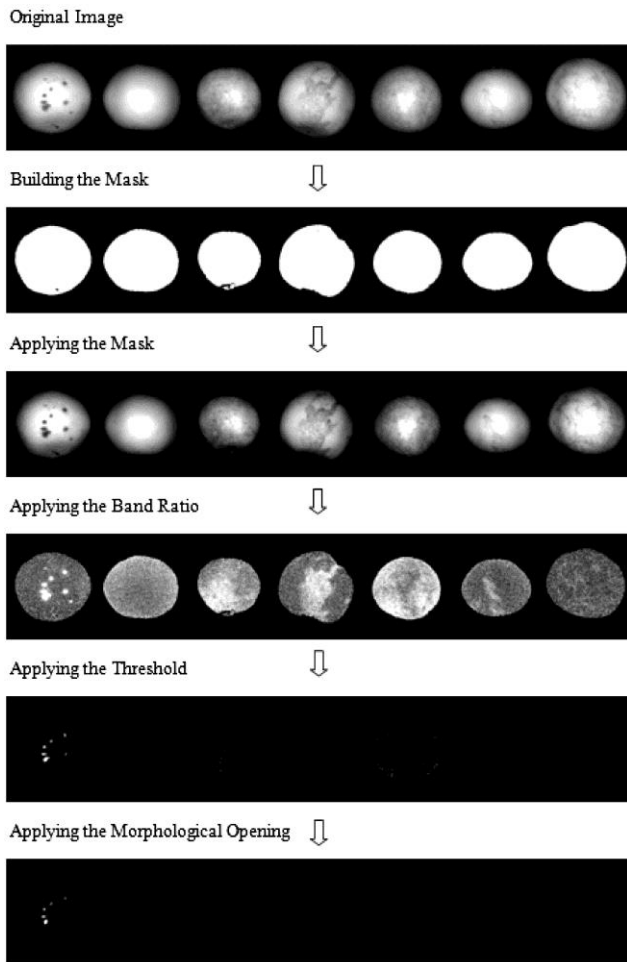


Figure 4 Classification Method-Discrimination of canker from other peel conditions clearly portrays how the image processing algorithm discriminates between canker and other disease conditions

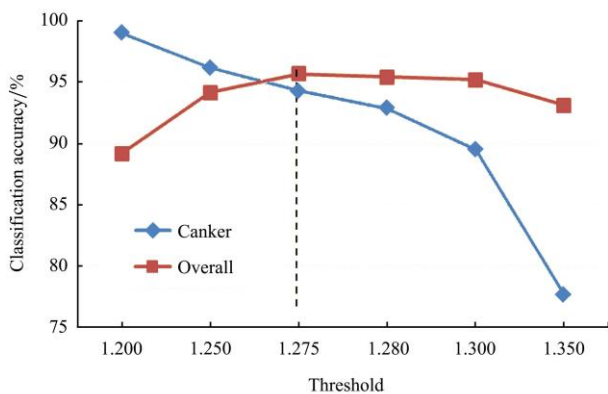


Figure 5 Effect of variation of threshold values demonstrating how canker classification accuracy and the overall classification accuracy show opposite trends. In order to achieve an optimal performance a tradeoff in the threshold value is necessary.

A threshold of 1.275 gives the best results

It can be concluded that canker classification accuracy diminishes with increasing threshold value due to filtering out the smallest canker lesions; on the other hand, the overall accuracy shows opposite trend of increasing with threshold value. However, after a certain threshold value, the overall accuracy also starts dropping as canker misclassification increases at higher threshold values. The threshold value of 1.275 appears to give best tradeoff between canker classification accuracy (94.3%) and overall classification (95.7%). However, depending on the preferences of the packinghouse and import/export rules, it would be possible to sacrifice overall classification accuracy to improve canker detection. Table 2 summarizes these classification results for the two band ratio methods.

Table 2 Summary of classification results

Disease	Number of samples	Rule classifier threshold	Number of misclassified	Classification accuracy/%
Canker	210	1.275	12*	94.3
Greasy spot	120	1.275	12	90.0
Insect damage	60	1.275	1	98.3
Melanose	180	1.275	10	94.4
Scab	180	1.275	5	97.2
Wind scar	60	1.275	0	100.0
Market	150	1.275	1	99.3
Overall	960		41	95.7

Note: * Represents the number of misclassified canker samples out of the total of 210 canker infected samples.

When evaluating lesion detection size limits, one should know that along with the number of erosion cycles, excessively high values of threshold can also result in increased misclassification and thus poor estimation of the size of the smallest detectable canker lesion.

3.2 Binary lesion size estimation

After classifying all citrus fruits as either “canker” or “no canker”, the MATLAB algorithm (using ‘bwareaopen’) was applied to detect the smallest cankerous lesion. Figure 6 shows the zoomed images of the same sample as in Figure 3, before and after applying the ‘bwareaopen’ function. As can be seen, the two smallest lesions detected by the algorithm in the left image have disappeared in the right image due to application of ‘bwareaopen’. The application of erosion in the opening filter should not be confused with the use

of 'bwareaopen'. The morphological opening filter is used to remove unwanted pixels from edges and other minor peel conditions, and could be implemented in an online detection system. While the 'bwareaopen' function was used as an analysis tool to assist in detecting the smallest cankerous lesion present in the binary image.

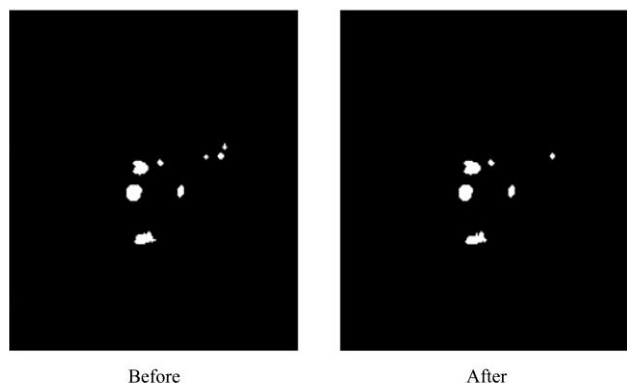


Figure 6 Final binary image of a sample before and after applying the 'bwareaopen' function. Note that two lesions in the left image have disappeared in the right image due to application of the function 'bwareaopen'. These two lesions were the smallest lesions detected by our algorithm

The two most important factors influencing the estimation of the smallest canker lesion present are 1) the

number of erosion cycles used in the morphological opening operation, and 2) the threshold value used in image classification. The effect of variation of threshold value on detectable lesion size was previously discussed in Figure 5, where it is demonstrated that as the threshold value increased small sized and lighter pigmented canker lesions were removed from the final binary image. This resulted in reduced classification accuracy because of increased false negative errors. The effect of the number of erosion cycles is explained by Table 3, which shows the classification accuracy for 210 cankerous grapefruit samples as erosion cycles varying and the threshold is held constant at 1.275. As erosion cycles are increased from 1 to 5, the classification results go from 94.3% down to 11.9%, respectively. Also when considering the smallest lesion (number of pixels) detected, the smallest detectable lesion size increases as erosion cycles increases. This is because small sized and lighter pigmented lesions are removed by additional erosion cycles. In this study, it was found that a single erosion cycle and a classification threshold of 1.275 provided the optimal canker lesion detection thus reducing false negative errors.

Table 3 Effect of number of erosion cycles on canker lesion size estimation

Number of erosion cycles	Number of misclassified samples*	Canker classification accuracy/%	No. of Pixels in smallest lesion	Equivalent area /mm ²	Equivalent diameter /mm
1	12	94.29	5	1.80	1.51
2	60	71.43	13	4.68	2.44
3	109	48.10	25	9.00	3.39
4	162	22.86	41	14.76	4.34
5	185	11.90	61	21.96	5.29

Note: * Represents the number of misclassified canker samples out of the total of 210 canker infected samples.

3.3 Mapping binary lesion size to original multispectral image

Figure 7 portrays the process of mapping the binary canker lesion to the original multispectral image. The center image highlights the detected lesion in binary image with a red circle, while the corresponding original lesion is encircled in the left image. The right image shows the selected lesion located in the original multispectral image with the region of interest (ROI) being grown (red in color) using ENVI's ROI tool. This tool will assist in calculating the number of pixels in the

actual canker lesion of interest in the multispectral image.

Each of the 210 cankerous grapefruit samples was examined and the smallest canker lesion was detected in the corresponding binary images and then mapped back to the original multispectral image. The plot in Figure 8 shows probability distribution of the actual canker lesion size. As can be seen most of the data is concentrated in the lesion size range from 6 to 35 pixels. This plot can be approximated by a 'Log-Normal' distribution, rather than a Normal or Gaussian distribution since the data set does not exhibit a central tendency.

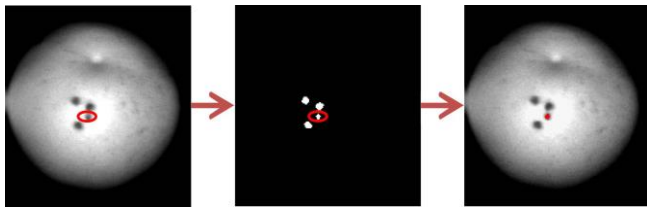


Figure 7 Mapping binary lesion size to original hyperspectral image. The encircled lesion in the left and the middle picture is mapped to actual image of the fruit to calculate the actual size of the lesion. The ENVI image processing software was used to find the actual lesion size

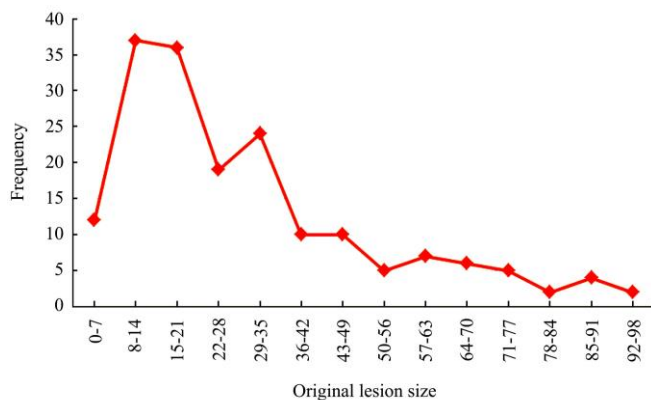


Figure 8 Probability distribution of lesion size of subset of all samples. Details of the encircled part in Figure 8 can be seen in this figure

We can also observe that the mode of the dataset corresponds to the lesion size range of 8 to 14 pixels with a frequency of occurrence of 37 out of 210, while 73 out of 210 would fall in the range of 8 to 21. This suggests that when using the optimal number of erosions and threshold, the two-band classification approach is consistently classifying lesions in this size range at above 94.0% accuracy.

The size of the smallest canker lesion, in terms of surface area (mm^2), was determined utilizing the spatial resolution of each pixel (0.6 mm in both horizontal and vertical directions) as:

$$\text{Area} = \text{Number of pixels in smallest lesion} \times 0.6 \text{ mm} \times 0.6 \text{ mm} \quad (2)$$

Assuming that the canker lesions can be approximated by a circular shape, the equivalent diameter of the smallest lesion can be calculated in mm. The smallest canker lesion detected consisted of 6 pixels. The surface area of corresponding lesion was 2.16 mm^2 and the corresponding equivalent diameter was 1.66 mm.

One other important point to be noted is that the original resolution of the image was not used to calculate the size of the smallest lesion. The size of the original 3-D hyperspectral image cube was $1740 \times 400 \times 92$ (92 bands) which was reduced to $870 \times 200 \times 92$ by image preprocessing to lessen the computation. This resulted in a reduction of the pixel resolution from $0.3 \times 0.3 \text{ mm}^2$ to $0.6 \times 0.6 \text{ mm}^2$. If the original pixel resolution of $0.3 \times 0.3 \text{ mm}^2$ were used, then it could be inferred that smaller sized canker lesions could be detected, but at the cost of increased computation time and memory usage.

4 Conclusions

This research focused on determining the lower limit for detecting small canker lesions for rapid real time applications. Multispectral reflectance imaging was found capable of detecting very small citrus canker lesions when utilizing a band ratio with wavelengths of 834 nm and 729 nm. The threshold value of 1.275 along with a single erosion cycle in the opening filter gave the optimum classification accuracy. It was observed that smaller values of thresholds gave better canker classification accuracy (up to 99.0%), while giving a lower overall accuracy (89.0%). The best overall classification accuracy was found to be 95.7%.

Canker lesions as small as 6 pixels in size (effective surface area of 2.16 mm^2) were accurately classified, corresponding to an equivalent diameter was 1.66 mm. The pixel resolution used in this study was $0.6 \times 0.6 \text{ mm}^2$. If higher resolution images were used it is possible that even smaller canker lesions could be detected, but at the cost of computational requirement and hardware expense. However, depending on import/export lesion size limits, this could be a viable option in certain cases. The canker lesion detection and sizing approach described in this study provides a simple and reliable methodology for establishing minimum detectable lesion size with a detection accuracy of more than 95.0%.

Acknowledgements

The authors gratefully acknowledge the financial support of Florida Fresh Packer Association and USDA Technical Assistance for Specialty Crops. The authors

would also like to thank Dr. Moon Kim and Dr. Kuanglin Chao from USDA-ARS Environmental Microbial and Food Safety Laboratory, and Mr. Mike Zingaro and Mr. Greg Pugh from University of Florida, for their help in building the hyperspectral imaging system.

[References]

- [1] Schubert T S, Miller J W, Gabriel D W. Another outbreak of bacterial canker on citrus in Florida. *Plant Disease*, 1996; 80(10): 1208.
- [2] Qin J W, Burks T F, Ritenour M A, Bonn W G. Detection of citrus canker using hyperspectral reflectance imaging with spectral information divergence. *Journal of Food Engineering*, 2009; 93(2): 183-191.
- [3] Qin J W, Burks T F, Kim M S, Chao K, Ritenour M A. Citrus canker detection using hyperspectral reflectance imaging and PCA-based image classification method. *Sensing and Instrumentation for Food Quality and Safety*, 2008; 2(3): 168-177.
- [4] USDA APHIS. Citrus Canker: Movement of Fruit from Quarantined Areas. *Federal Register: Rules and Regulations*, 2009; 74(203): 54431-54445.
- [5] Miller W M, Drouillard G P. Multiple feature analysis for machine vision grading of Florida citrus. *Applied Engineering in Agriculture*, 2001; 17(5): 627-633.
- [6] Pydipati R, Burks T F, Lee W S. Identification of citrus disease using color texture features and discriminant analysis. *Computers and Electronics in Agriculture*, 2006; 52(1-2): 49-59.
- [7] Blasco J, Aleixos N, Gómez J, Moltó E. Citrus sorting by identification of the most common defects using multispectral computer vision. *Journal of Food Engineering*, 2007; 83(3): 384-393.
- [8] Gómez-Sanchis J, Moltó E, Camps-Valls G, Gómez-Chova L, Aleixos N, Blasco J. Automatic correction of the effects of the light source on spherical objects. An application to the analysis of hyperspectral images of citrus fruits. *Journal of Food Engineering*, 2008; 85(2): 191-200.
- [9] Qin J W, Burks T F, Zhao X H, Niphadkar N, Ritenour M A. Hyperspectral band selection for multispectral detection of citrus canker. *Transactions of ASABE*, 2011; 54(6): 1-11.
- [10] Kim M S, Chen Y R, Mehl P M. Hyperspectral reflectance and fluorescence imaging system for food quality and safety. 2001, ASAE ISSN 0001-2351.
- [11] Kim M S, Lefcourt A M, Chao K, Chen Y R, Kim I, Chan D E. Multispectral detection of fecal contamination on apples based on hyperspectral imagery: Part I. Application of visible and near-infrared reflectance imaging. *Transactions of ASAE*, 2002; 45(6): 2027- 2037.
- [12] Qin J W, Burks T F, Zhao X H, Niphadkar N, Ritenour M A. Development of a two-band spectral imaging system for real-time citrus canker detection. *Journal of Food Engineering*, 2012, 108(1): 87-93.
- [13] Timmer L W, Garnsey S M, Graham J H. *Compendium of Citrus Diseases (Second Edition)*. 2000, the American Phytopathological Society, St. Paul, MN, USA.